A Journal of the Gesellschaft Deutscher Chemiker

Angewandte International Edition GDCh Chemie

www.angewandte.org

## Accepted Article

**Title:** A Hybrid Platform Based on a Bispecific Peptide-Antibody Complex for Targeted Cancer Therapy

**Authors:** Byeongjun Yu, Dobeen Hwang, Hyungsu Jeon, Hyungjun Kim, Yonghyun Lee, Hyeongseop Keum, Jinjoo Kim, Dong Yun Lee, Yujin Kim, Junho Chung, and Sangyong Jon



**To be cited as:** *Angew. Chem. Int. Ed.* 10.1002/anie.201811509
*Angew. Chem.* 10.1002/ange.201811509

**Link to VoR:** http://dx.doi.org/10.1002/anie.201811509
http://dx.doi.org/10.1002/ange.201811509

WILEY-VCH

10.1002/anie.201811509

WILEY-VCH

COMMUNICATION

# A Hybrid Platform Based on a Bispecific Peptide-Antibody Complex for Targeted Cancer Therapy

Byeongjun Yu[a], Dobeen Hwang[d], Hyungsu Jeon[a], Hyungjun Kim[a], Yonghyun Lee[a], Hyeongseop Keum[a], Jinjoo Kim[a], Dong Yun Lee[b], Yujin Kim[a], Junho Chung[d], and Sangyong Jon*[a],[b],[c]

**Abstract:** Peptide-based therapeutics have suffered from a short plasma half-life. On the other hand, antibodies suffer from poor penetration in solid tumors owing to their large size. Here, we present a new molecular form—a hybrid complex between a hapten-labeled bispecific peptide and an anti-hapten antibody, designated HyPEP-body—that may be able to overcome the aforementioned limitation. A bispecific peptide containing a cotinine tag was synthesized by linking a peptide specific to fibronectin extra domain B (EDB) and a peptide able to bind and inhibit vascular endothelial growth factor (VEGF), yielding cot-biPEP$_{EDB\text{-}VEGF}$. Simple mixing of cot-biPEP$_{EDB\text{-}VEGF}$ and anti-cotinine antibody (Ab$^{cot}$) yielded the hybrid complex, HyPEP$_{EDB\text{-}VEGF}$. The HyPEP$_{EDB\text{-}VEGF}$ retained the characteristics of the included peptides, and showed improved pharmacokinetic behavior. Moreover, The HyPEP$_{EDB\text{-}VEGF}$ showed tumor growth inhibition with excellent tumor accumulation and penetration. These findings suggest that the newly developed hybrid platform described here offers a solution for most peptide therapeutics that suffer from a short circulation half-life in blood.

While antibody-based biologics have achieved great success in treating various diseases in the last two decades,[1] the broader use of peptide-based therapeutics has been limited by the short plasma half-life of these agents, reflecting their rapid proteolysis and renal clearance in *vivo*.[2] These limitations of peptide therapeutics have spawned recent efforts to develop alternatives based on the concept of hybrids between peptides and antibodies. Two representative approaches are 'Peptibody' and 'CovX-body'. In the peptibody platform, therapeutic peptides are grafted to an Fc domain, not to an entire antibody, and expressed as a fusion protein. AMG-386, a peptibody that targets both angiopoietin 1 (ANGPT1) and ANGPT2, is now undergoing Phase III clinical trials as a combination therapy with chemotherapeutic agents.[3] The molecular format of CovX-body relies on site-specific covalent conjugation of therapeutic peptides to two antigen-binding sites (Fab arms) of an antibody. CVX-241, a CovX-body that consists of bispecific peptide inhibitors against vascular endothelial growth factor (VEGF) and ANGPT2 linked chemically to an antibody, had entered clinical trials years ago, but unfortunately failed to show improvement in therapeutic index.[4] Although the two aforementioned platforms significantly extended the plasma half-life of the peptide therapeutics because of the presence of Fc, they still suffered the same limited tumor penetration that plagues conventional antibody therapeutics. Furthermore, significant technology-specific variability—the expression level of each individual peptibody for a particular disease target in the case of peptibody technology, and the conjugation yield of the peptides to an antibody for CovX-body technology—poses hurdles in the manufacturing process. Hence, a new molecular platform that can extend plasma half-life and also improve tumor penetration of peptide therapeutics is needed.

Here, we present a new molecular platform based on a hybrid complex between a bispecific peptide and an antibody, designated HyPEP-body, consisting of two hapten-labeled bispecific peptides and an anti-hapten antibody. Cotinine, a major metabolite of nicotine, and anti-cotinine antibody (Ab$^{cot}$) were used in this study as a model hapten and hapten-specific antibody, respectively.[5] It has been shown that Ab$^{cot}$ can extend the plasma half-life of a cotinine-labeled aptamer.[6] As depicted in Figure 1, a key difference in the molecular format of a HyPEP-body compared with a bispecific CovX-body is that the peptide pharmacophore in a HyPEP-body is bound to the antigen-binding site of an antibody in a non-covalent manner, like avidin-biotin interactions. This molecular feature may prolong the plasma half-life of the bispecific peptide owing to the presence of an intact form of the antibody while allowing dissociation of the peptide from the HyPEP-body, thereby enhancing tumor penetration. As a proof-of-concept study, we constructed a HyPEP-body using a cotinine (cot)-labeled bispecific peptide targeting EDB and VEGF (cot-biPEP$_{EDB\text{-}VEGF}$) and Ab$^{cot}$, yielding the hybrid complex, HyPEP$_{EDB\text{-}VEGF}$. EDB is specifically over-expressed in several types of malignant tumors,[7] and thus is considered a promising target for cancer imaging and therapy.[8] Moreover, the association of VEGF signaling with survival, migration, apoptosis and metastasis of tumor cells[9] has made this signaling axis a natural target for the development of inhibitors, several of which are used clinically for treatment of many kinds of cancers.[10] Thus, we hypothesized that HyPEP$_{EDB\text{-}VEGF}$ with enhanced blood circulation would specifically target EDB-overexpressing tumors and inhibit abnormal VEGF function within the tumor microenvironment (Figure 1). We found that the binding specificity and activity of the two peptides towards their respective targets were preserved in HyPEP$_{EDB\text{-}VEGF}$. The circulation time of the pharmacophore peptide in blood also increased dramatically upon complexation with Ab$^{cot}$ in the form of a HyPEP-body. Moreover, the released cot-biPEP$_{EDB\text{-}VEGF}$ was distributed more widely and deeply in tumor tissue. Finally, HyPEP$_{EDB\text{-}VEGF}$ effectively inhibited the growth of a human glioblastoma xenograft in mice.

[a] B. Yu, Dr. H. Jeon, Dr. H. Kim, Dr. Y. Lee, H. Keum, J. Kim, Y. Kim, Prof. Dr. S. Jon
KAIST Institute for the BioCentury, Department of Biological Sciences
Korea Advanced Institute of Science and Technology (KAIST)
291 Daehak-ro, Daejeon 34141, Republic of Korea
E-mail : syjon@kaist.ac.kr

[b] Dr. D.Y. Lee, Prof. Dr. S. Jon
Graduate School of Medical Science and Engineering
KAIST, 291 Daehak-ro, Daejeon 34141, Republic of Korea

[c] Prof. Dr. S. Jon
Center for Precision Bio-Nanomedicine
KAIST, 291 Daehak-ro, Daejeon 34141, Republic of Korea

[d] Dr. D. Hwang, Prof. Dr. J. Chung
Department of Biochemistry and Molecular Biology
Seoul National University College of Medicine
103 Daehak-ro, Seoul 03080, Republic of Korea

10.1002/anie.201811509

WILEY-VCH

COMMUNICATION

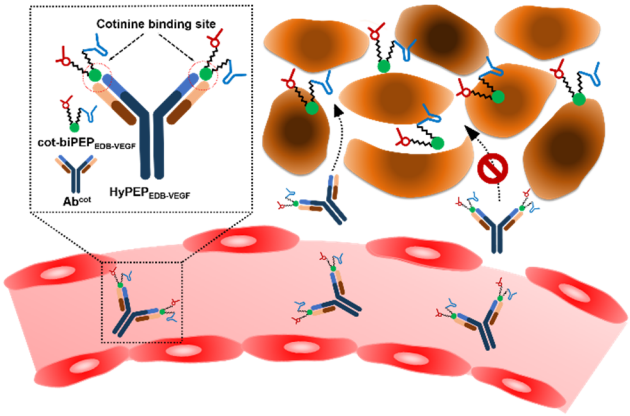


**Figure 1.** Graphical abstract of the unique features of the HyPEP-body, and schematic depiction of the HyPEP-body prototype, HyPEP$_{EDB-VEGF}$.

A bispecific peptide targeting both EDB and VEGF was synthesized by conjugating the corresponding EDB- and VEGF-binding peptides using an appropriate linker, as illustrated in Scheme 1. An aptide—a novel class of high-affinity and -specificity peptides developed by our group—specific for EDB (APT$_{EDB}$),[11] and a VEGF-binding high-affinity peptide (PEP$_{VEGF}$)[12] were chosen for synthesis of the desired cotinine tag-labeled bispecific peptide (cot-biPEP$_{EDB-VEGF}$). First, the lysine residue of PEP$_{VEGF}$ was reacted with a hydrophilic heterobifunctional linker to yield maleimide-functionalized PEP$_{VEGF}$. A hydrophilic linker containing both the cotinine tag and sulfhydryl group at one end was attached to the N-terminus of the EDB-binding aptide by solid phase peptide synthesis. Next, the two modified peptides were covalently linked to each other by reacting the maleimide and sulfhydryl functionalities in each peptide, yielding the bispecific peptide with a cotinine tag, cot-biPEP$_{EDB-VEGF}$. A non-relevant aptide with a scrambled sequence (APT$_{SCR}$) was used to prepare a control bispecific peptide (cot-biPEP$_{SCR-VEGF}$) that does not target EDB. Chemical structures and names of all peptides used in this study are shown in Figure S1. All modified peptides obtained in this study were purified by high performance liquid chromatography (HPLC; Figure S2) and their molecular masses were analyzed by matrix assisted laser desorption ionization-time of flight mass spectrometry (MALDI-TOF MS; Figure S3). The purity of cot-biPEP$_{EDB-VEGF}$ and cot-biPEP$_{SCR-VEGF}$ determined by HPLC was 98.5% and 98.6%, respectively (Figure S4). Finally, the hybrid complex between the bispecific peptide and Ab$^{cot}$ (HyPEP$_{EDB-VEGF}$) was formed by simply mixing the two components at a 2:1 molar ratio at ambient temperature in buffer solution.[6]

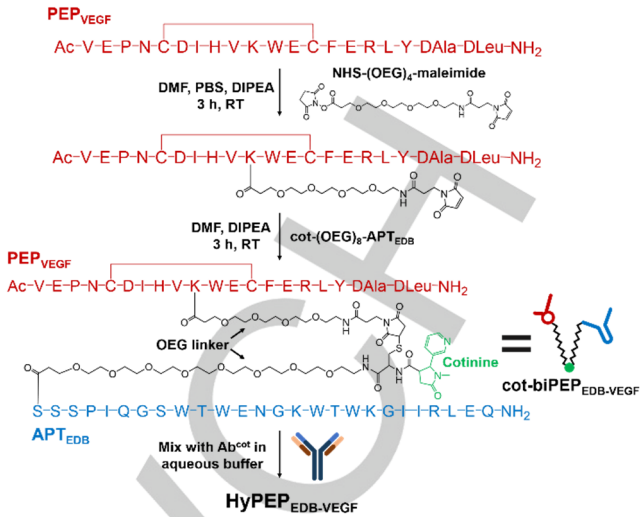


**Scheme 1.** A schematic illustration for the synthesis of cot-biPEP$_{EDB-VEGF}$ and the preparation of HyPEP$_{EDB-VEGF}$

To determine whether HyPEP$_{EDB-VEGF}$ retained its target specificity, we performed ELISAs for each target. HyPEP$_{EDB-VEGF}$ showed concentration-dependent specific binding to human VEGF (hVEGF; Figure 2a) and EDB (Figure 2b). Although PEP$_{VEGF}$ was identified from screening against hVEGF,[13] we found that HyPEP$_{EDB-VEGF}$ was also able to bind mouse VEGF (mVEGF; Figure 2c) presumably due to the high homology (~90%) between hVEGF and mVEGF.[14] We further found that HyPEP$_{EDB-VEGF}$ was able to bind both targets simultaneously in ELISAs for immobilized EDB and soluble biotinylated hVEGF, respectively (Figure 2d). The affinities of HyPEP$_{EDB-VEGF}$ were measured by surface plasmon resonance (SPR) instrument. The dissociation constant ($K_d$) of HyPEP$_{EDB-VEGF}$ for hVEGF and mVEGF were ~4.4 nM and ~14 nM respectively (Figure S5a,b). The $K_d$ of HyPEP$_{EDB-VEGF}$ for EDB was ~32 nM (Figure S5c), which is even lower than that of the unmodified original APT$_{EDB}$ (~65 nM); this increased affinity might reflect a "bivalent" (dimer) effect of the peptide displayed on the HyPEP-body. These results clearly

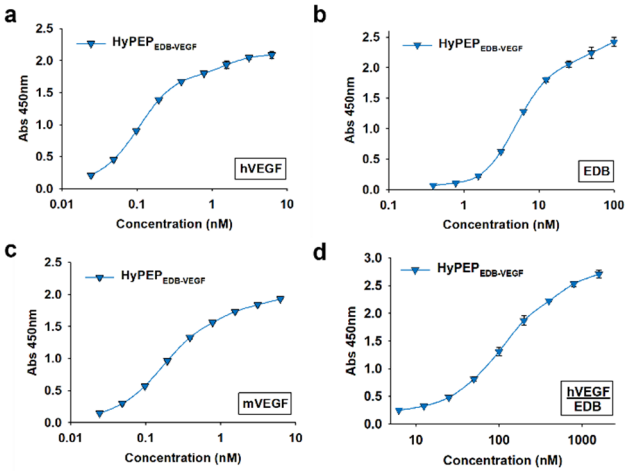


indicate that the target-binding specificity and affinity of the bispecific peptide (biPEP$_{EDB-VEGF}$) are preserved, even after complex formation with Ab$^{cot}$.

**Figure 2.** Characterization of HyPEP$_{EDB-VEGF}$ at the protein level. Direct binding ELISA of HyPEP$_{EDB-VEGF}$ against a) hVEGF, b) EDB, and c) mVEGF. d)

10.1002/anie.201811509





HyPEP$_{EDB-VEGF}$ was allowed to bind to the immobilized EDB, followed by treatment with biotinylated hVEGF and detection with streptavidin-horseradish peroxidase. Representative results of two experiments are shown.

We next examined the specificity of the HyPEP-body using EDB-positive cancer cells. U87MG human glioblastoma cells and PC3 human prostate cancer cells were used as EDB-positive and -negative cancer cell lines, respectively. The expression level of EDB in each cell line was measured by conventional reverse transcription-polymerase chain reaction (RT-PCR) and quantitative RT-PCR, the latter of which revealed ~80-fold higher expression of EDB in U87MG cells than in PC3 cells (Supporting Information, Figure S6). To image specific cell binding, we first treated both cancer cell lines with HyPEP$_{EDB-VEGF}$ and then with a fluorescent dye-labeled secondary antibody for Ab$^{cot}$. A strong fluorescence signal was observed around the cell membrane of EDB-positive U87MG cells (Figure 3a), but little signal was detected in EDB-negative PC3 cells (Figure 3b). We next examined whether HyPEP$_{EDB-VEGF}$ was capable of inhibition VEGF function by performing proliferation and tube-formation assays with HUVECs. HyPEP$_{EDB-VEGF}$ effectively suppressed VEGF-induced cell proliferation (Figure 3c) and tube formation (Figure 3d and Figure S7). Taken together, these results clearly suggest that HyPEP$_{EDB-VEGF}$ retains target-binding specificity and biological activity.

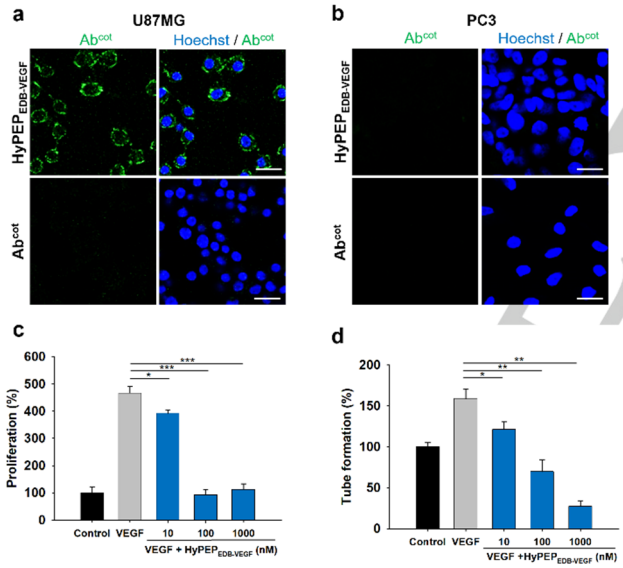


**Figure 3.** Confirmation of HyPEP$_{EDB-VEGF}$ binding to EDB and inhibition of VEGF at the cell level. a,b) Confocal microscopy images of EDB-positive U87MG cells and EDB-negative PC3 cells after treatment with HyPEP$_{EDB-VEGF}$, followed by incubation with a secondary antibody for Ab$^{cot}$. Scale bar: 50 μm. c,d) Quantitative analysis of VEGF-induced proliferation and tube formation in HUVECs after incubation with hVEGF or hVEGF plus HyPEP$_{EDB-VEGF}$. (n = 5; *, $P < 0.05$; **, $P < 0.01$; ***, $P < 0.001$)

The stability of cot-biPEP$_{EDB-VEGF}$ and HyPEP$_{EDB-VEGF}$ in serum was assessed by incubation in mouse serum for varying lengths of time. An ELISA against hVEGF or EDB was used to determine the concentration of the active form of cot-biPEP$_{EDB-VEGF}$ remaining in samples. At 48 h post incubation, the remaining binding activity of cot-biPEP$_{EDB-VEGF}$ and HyPEP$_{EDB-VEGF}$ was 34.5% versus 73.1% for VEGF and 19.9% versus 43.4% for EDB, respectively (Figure 4a; Figure S8a). These results suggest that complexation with Ab$^{cot}$ protects the peptide from proteolytic degradation, resulting in increased stability in serum. In addition, the stability of HyPEP$_{EDB-VEGF}$ was also evaluated in human serum. The remaining binding activity of HyPEP$_{EDB-VEGF}$ at 48 h post incubation was 58.7 % for VEGF and 50.4 % for EDB, indicating that HyPEP$_{EDB-VEGF}$ is also stable in human serum (Figure S8b).

Next, we carried out a pharmacokinetics study of cot-biPEP$_{EDB-VEGF}$ and HyPEP$_{EDB-VEGF}$ after intraperitoneal (I.P.) injection. Blood was drawn via retro orbital puncture at predetermined time points, and the concentration of cot-biPEP$_{EDB-VEGF}$ in blood samples was determined by ELISA against hVEGF (Figure 4b). The key pharmacokinetic parameters are shown in Table 1. Using a non-compartment model, we calculated the clearance half-life ($t_{1/2}$) of HyPEP$_{EDB-VEGF}$ in blood to be ~23.4 h, which was considerably greater than that of cot-biPEP$_{EDB-VEGF}$ (~1.2 h). The area under the plasma concentration-time curve from time zero to infinity ($AUC_{0-\infty}$) of HyPEP$_{EDB-VEGF}$ was also significantly greater than that of cot-biPEP$_{EDB-VEGF}$ alone (~603 vs. 61). These results clearly indicate that complexation of cot-biPEP$_{EDB-VEGF}$ with Ab$^{cot}$ (HyPEP$_{EDB-VEGF}$) results in a dramatic extension of the plasma half-life of the peptide therapeutic. In addition, the time to reach maximum plasma concentration ($t_{max}$) also increased, suggesting that complexation with Ab$^{cot}$ delayed absorption of the I.P. injected peptide from the systemic circulation.

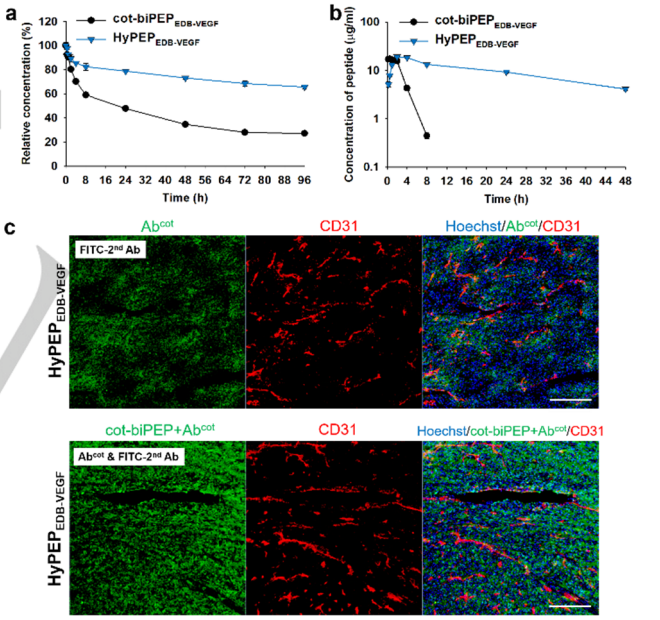


**Figure 4.** Pharmacokinetics and distribution of HyPEP$_{EDB-VEGF}$ in tumor tissues. a) Stability of cot-biPEP$_{EDB-VEGF}$ and HyPEP$_{EDB-VEGF}$ in mouse serum was evaluated via ELISA against hVEGF (n = 2). b) Determination of the cot-biPEP$_{EDB-VEGF}$ concentration in collected serum samples at different time points after I.P. injection of cot-biPEP$_{EDB-VEGF}$ or HyPEP$_{EDB-VEGF}$ (n = 5). c) Confocal microscopy images of tumor tissues after I.P. injection of HyPEP$_{EDB-VEGF}$. Ab$^{cot}$ only was detected by staining tumor sections with anti-CD31 antibody and human IgG isotype control antibody, followed by incubation with fluorescence-conjugated secondary antibodies for anti-CD31 antibody and Ab$^{cot}$. Both released cotinine-labeled peptide and Ab$^{cot}$ were detected by adding Ab$^{cot}$ instead of human IgG isotype control antibody. Scale bar: 200 μm.

10.1002/anie.201811509





**Table 1.** Pharmacokinetic parameters of cot-biPEP$_{EDB\text{-}VEGF}$ in BALB/c nude mice after I.P. injection of cot-biPEP$_{EDB\text{-}VEGF}$ or HyPEP$_{EDB\text{-}VEGF}$ (n = 5).

| Parameter | cot-biPEP$_{EDB\text{-}VEGF}$ | HyPEP$_{EDB\text{-}VEGF}$ |
|---|---|---|
| $t_{1/2}$ (h) | 1.18 | 23.4 |
| $t_{max}$ (h) | 0.50 | 2.00 |
| $C_{max}$ (μg mL$^{-1}$) | 17.1 | 19.1 |
| AUC$_{0\text{-}\infty}$ (μg·h mL$^{-1}$) | 61.0 | 602.9 |

$t_{1/2}$, clearance half-life; $t_{max}$, time to reach maximum plasma concentration; $C_{max}$, maximum plasm drug concentration; AUC$_{0\text{-}\infty}$, area under the plasma concentration-time curve from time zero to infinity.

Accumulation and distribution of HyPEP$_{EDB\text{-}VEGF}$ in tumor tissue were examined by immunohistochemistry. Staining for HyPEP$_{EDB\text{-}VEGF}$ using FITC-2$^{nd}$ Ab showed strong fluorescence around perivascular regions of the tumor, whereas staining for both HyPEP$_{EDB\text{-}VEGF}$ and the released cot-biPEP$_{EDB\text{-}VEGF}$ showed a much more uniform distribution in the tumor section (Figure 4c). This result suggests that cot-biPEP$_{EDB\text{-}VEGF}$ was released from Ab$^{cot}$ and subsequently penetrated deeper into the tumor. In contrast, I.P. injection of Ab$^{cot}$ alone or HyPEP$_{SCR\text{-}VEGF}$ lacking EDB-targeting ability showed much lower accumulation in the tumor (Figure S9). Next, the tissue distribution of HyPEP$_{EDB\text{-}VEGF}$ was determined by measuring the amount of bispecific peptide in each tissue extract using ELISA. The amount of the peptide accumulated in the tumor was approximately two fold higher than that of normal tissues; however, HyPEP$_{SCR\text{-}VEGF}$ showed little preferential accumulation in the tumor compared to normal tissues (Figure S10).

Encouraged by the favorable features of HyPEP$_{EDB\text{-}VEGF}$, including prolonged circulation in the blood and deep penetration in tumors, we examined the antitumor efficacy of HyPEP$_{EDB\text{-}VEGF}$ in a U87MG mouse xenograft model. This tumor model was selected because U87MG cells express high levels of EDB and are highly sensitivity to anti-VEGF agents.[15] When tumor volumes reached approximately 100 mm$^3$, mice received each experimental agent via I.P. injection every other day for 14 d. Tumor growth and changes in body weight were monitored every 2 days. As shown in Figure 5a and Figure S11a, tumor growth was substantially inhibited by HyPEP$_{EDB\text{-}VEGF}$ (75.9% relative to PBS-treated control group). In contrast, tumor growth inhibition was not significantly different between cot-biPEP$_{EDB\text{-}VEGF}$ and PBS control groups, despite a trend toward greater inhibition in the cot-biPEP$_{EDB\text{-}VEGF}$ group. We speculate that the greatly enhanced antitumor efficacy of HyPEP$_{EDB\text{-}VEGF}$ compared with the peptide alone may be attributable to the prolonged plasma half-life and increase resistance proteolysis, and thus greater accumulation and distribution in the tumor. Next, to investigate the EDB-targeting effect of HyPEP$_{EDB\text{-}VEGF}$, we replaced the EDB-binding aptide with a scrambled aptide, yielding HyPEP$_{SCR\text{-}VEGF}$, which is unable to recognize EDB. We also prepared a HyPEP-body lacking the VEGF-binding peptide, designated HyPEP$_{EDB}$, as an additional control to investigate the biological effects of the EDB-binding aptide. Treatment with HyPEP$_{EDB}$ had little effect on tumor growth, whereas HyPEP$_{SCR\text{-}VEGF}$ lacking EDB-targeting ability showed appreciable tumor growth inhibition (43.4% relative to PBS-treated group); however, EDB-targeted HyPEP$_{EDB\text{-}VEGF}$ showed much greater antitumor efficacy than HyPEP$_{SCR\text{-}VEGF}$ (52.7% relative to HyPEP$_{SCR\text{-}VEGF}$; Figure 5b; Figure S11b). These results suggest that both the EDB-binding aptide and Ab$^{cot}$ have little anticancer activity in their own right, and that the resulting antitumor efficacy observed for both HyPEP$_{SCR\text{-}VEGF}$ and HyPEP$_{EDB\text{-}VEGF}$ is mainly attributable to the VEGF-binding peptide. The appreciable antitumor efficacy of HyPEP$_{SCR\text{-}VEGF}$ may reflect passive accumulation of the HyPEP-body in the tumor by virtue of a greater enhanced permeability and retention (EPR) effect due to pro-longed circulation in the bloodstream. Because of its EDB-targeting ability, however, HyPEP$_{EDB\text{-}VEGF}$ exhibits significantly increased antitumor efficacy by more efficiently delivering the VEGF antagonist peptide into the tumor. None of the HyPEP-bodies tested in this study induced weight loss (Figure S12a,b), suggesting little apparent toxicity of the peptide-antibody hybrid system. To examine the mode of action of HyPEP$_{EDB\text{-}VEGF}$ in inhibiting tumor growth, we extracted tumors at the end of treatments and performed a vascularization analysis on tumor sections immunostained with an anti-CD31 antibody (Figure 5c,d). Treatment with HyPEP$_{EDB\text{-}VEGF}$ substantially reduced vessel density in tumors. For example, compared with PBS and HyPEP$_{SCR\text{-}VEGF}$ groups, HyPEP$_{EDB\text{-}VEGF}$ reduced vessel density by 50.8% and 26.3%, respectively, which was in good agreement with the results of tumor growth inhibition. These results suggest that HyPEP$_{EDB\text{-}VEGF}$ exhibits antitumor efficacy by inhibiting VEGF-induced tumor angiogenesis.

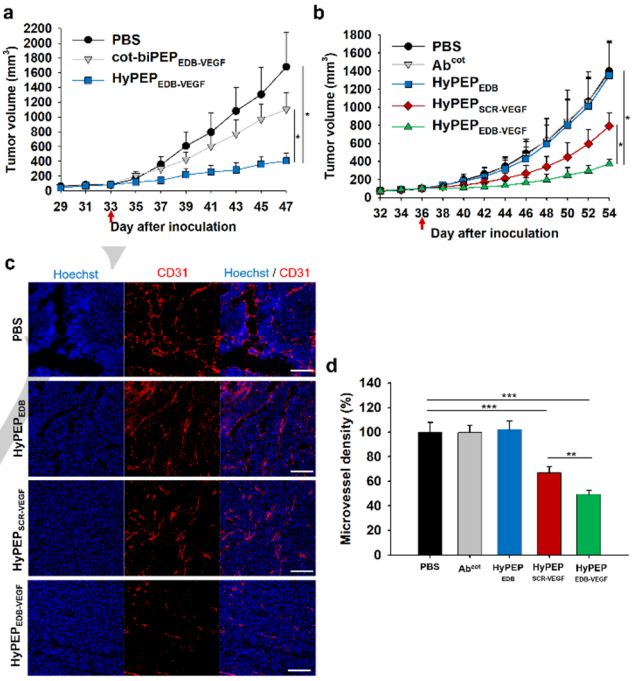


**Figure 5.** The antitumor activity of each therapeutic regimen in a U87MG mouse xenograft model. a) Changes of tumor size in U87MG tumor-bearing mice treated by I.P. injection of PBS, cot-biPEP$_{EDB\text{-}VEGF}$, or HyPEP$_{EDB\text{-}VEGF}$. b) Changes of tumor size in U87MG tumor-bearing mice treated by I.P. injection of PBS, Ab$^{cot}$, HyPEP$_{EDB}$, HyPEP$_{SCR\text{-}VEGF}$, or HyPEP$_{EDB\text{-}VEGF}$ (n = 5; *, $P < 0.05$). Red arrows indicate the injection start date. c) Slides of tumor sections obtained at the end of treatment with each regimen were immunostained with an anti-CD31 antibody, and counterstained with Hoechst dye to stain nuclei. Scale bar: 200 μm. d) Quantification of microvessel density in tumor sections (n = 15, 5 fields per section from 3 tumors per group; **, $P < 0.01$; ***, $P < 0.001$).

In summary, we developed a new type of hybrid molecular platform joining a peptide and an antibody that is designed to overcome a key shortcoming of peptide therapeutics—their short circulation half-life. Unlike previously developed hybrid platforms, the peptide-antibody hybrid developed herein, designated HyPEP-body, was formed

through non-covalent interactions between hapten-labeled bispecific peptides and the anti-hapten antibody. A model HyPEP-body that simultaneously binds to EDB and VEGF ($HyPEP_{EDB\text{-}VEGF}$) could extend the plasma half-life and significantly improve the tumor accumulation and distribution of peptide therapeutics. Importantly, the HyPEP-body significantly inhibited tumor growth in a U87MG mouse xenograft model. Taken together, our results suggest that the new peptide-antibody hybrid platform described here represents a solution to the problem of short duration of action that is characteristic of most peptide therapeutics.

## Acknowledgements

This work was supported by grants from the Basic Science Research Program through the National Research Foundation of Korea (NRF) funded by the Ministry of Science and ICT (Leading Researcher Program: NRF-2018R1A3B1052661) and Global Ph.D. Fellowship Pro-gram (No. 2015H1A2A1032806) through (NRF) funded by the Ministry of Education.

**Keywords:** Anti-cotinine antibody • Aptides • Cancer therapy • Extra domain B of fibronectin • Peptide therapeutics

[1] a) A. M. Scott, J. D. Wolchok, L. J. Old, *Nat Rev Cancer* **2012**, *12*, 278-287; b) G. J. Weiner, *Nat Rev Cancer* **2015**, *15*, 361-370.

[2] L. Diao, B. Meibohm, *Clin Pharmacokinet* **2013**, *52*, 855-868.

[3] J. Oliner, H. Min, J. Leal, D. Yu, S. Rao, E. You, X. Tang, H. Kim, S. Meyer, S. J. Han, N. Hawkins, R. Rosenfeld, E. Davy, K. Graham, F. Jacobsen, S. Stevenson, J. Ho, Q. Chen, T. Hartmann, M. Michaels, M. Kelley, L. Li, K. Sitney, F. Martin, J. R. Sun, N. Zhang, J. Lu, J. Estrada, R. Kumar, A. Coxon, S. Kaufman, J. Pretorius, S. Scully, R. Cattley, M. Payton, S. Coats, L. Nguyen, B. Desilva, A. Ndifor, I. Hayward, R. Radinsky, T. Boone, R. Kendall, *Cancer Cell* **2004**, *6*, 507-516.

[4] V. R. Doppalapudi, J. Huang, D. Liu, P. Jin, B. Liu, L. Li, J. Desharnais, C. Hagen, N. J. Levin, M. J. Shields, M. Parish, R. E. Murphy, J. Del Rosario, B. D. Oates, J. Y. Lai, M. J. Matin, Z. Ainekulu, A. Bhat, C. W. Bradshaw, G. Woodnutt, R. A. Lerner, R. W. Lappe, *Proc Natl Acad Sci U S A* **2010**, *107*, 22611-22616.

[5] S. Park, D. H. Lee, J. G. Park, Y. T. Lee, J. Chung, *Clin Chim Acta* **2010**, *411*, 1238-1242.

[6] K. Heo, S. W. Min, H. J. Sung, H. G. Kim, H. J. Kim, Y. H. Kim, B. K. Choi, S. Han, S. Chung, E. S. Lee, J. Chung, I. H. Kim, *J Control Release* **2016**, *229*, 1-9.

[7] a) P. Castellani, G. Viale, A. Dorcaratto, G. Nicolo, J. Kaczmarek, G. Querze, L. Zardi, *Int. J. Cancer* **1994**, *59*, 612-618; b) F. Oyama, S. Hirohashi, M. Sakamoto, K. Titani, K. Sekiguchi, *Cancer Res* **1993**, *53*, 2005-2011; c) K. Frey, M. Fiechter, K. Schwager, B. Belloni, M. J. Barysch, D. Neri, R. Dummer, *Exp Dermatol* **2011**, *20*, 685-688; d) G. V. P. Castellani, A. Dorcaratto, G. Nicolo, J. Kaczmarek, G. Querze, L. Zardi, *Int. J. Cancer* **1994**, *59*, 612-618; e) S. Sauer, P. A. Erba, M. Petrini, A. Menrad, L. Giovannoni, C. Grana, B. Hirsch, L. Zardi, G. Paganelli, G. Mariani, D. Neri, H. Durkop, H. D. Menssen, *Blood* **2009**, *113*, 2265-2274; f) T. Ohnishi, S. Hiraga, S. Izumoto, H. Matsumura, Y. Kanemura, N. Arita, T.Hayakawa, Hayakawa, *Clin Exp Metastasis* **1998**, *16*, 729-741.

[8] a) H. Kumra, D. P. Reinhardt, *Adv Drug Deliv Rev* **2016**, *97*, 101-110; b) P. E. Saw, S. Kim, I.h. Lee, J. Park, M. Yu, J. Lee, J.I. Kim, S. Jon, *Journal of Materials Chemistry B* **2013**, *1*, 4723-4726; c) P. E. Saw, J. Park, E. Lee, S. Ahn, J. Lee, H. Kim, J. Kim, M. Choi, O. C. Farokhzad, S. Jon, *Theranostics* **2015**, *5*, 746-754; d) G. Gu, Q. Hu, X. Feng, X. Gao, J. Menglin, T. Kang, D. Jiang, Q. Song, H. Chen, J. Chen, *Biomaterials* **2014**, *35*, 8215-8226; e) H. Kim, Y. Lee, I. H. Lee, S. Kim, D. Kim, P. E. Saw, J. Lee, M. Choi, Y. C. Kim, S. Jon, *J Control Release* **2014**, *178*, 118-124; f) D. Berndorff, S. Borkowski, S. Sieger, A. Rother, M. Friebe, F. Viti, C. S. Hilger, J. E. Cyr, L. M. Dinkelborg, *Clin Cancer Res* **2005**, *11*, 7053s-7063s; g) S. M. Rudman, M. B. Jameson, M. J. McKeage, P. Savage, D. I. Jodrell, M. Harries, G. Acton, F. Erlandsson, J. F. Spicer, *Clin Cancer Res* **2011**, *17*, 1998-2005; h) R. Locher, P. A. Erba, B. Hirsch, E. Bombardieri, L. Giovannoni, D. Neri, H. Durkop, H. D. Menssen, *J Cancer Res Clin Oncol* **2014**, *140*, 35-43.

[9] a) A. Hoeben, B. Landuyt, M. S. Highley, H. Wildiers, A. T. Van Oosterom, E. A. De Bruijn, *Pharmacol Rev* **2004**, *56*, 549-580; b) M. P. Barr, D. J. Bouchier-Hayes, J. J. Harmey, *Int. J. Oncol.* **2008**, *32*, 41-48; c) D. P. Lesslie, J. M. Summy, N. U. Parikh, F. Fan, J. G. Trevino, T. K. Sawyer, C. A. Metcalf, W. C. Shakespeare, D. J. Hicklin, L. M. Ellis, G. E. Gallick, *Br J Cancer* **2006**, *94*, 1710-1717; d) G. Pidgeon, J. Harmey, D. Foley, D. Bouchier-Hayes, *Br J Cancer* **2001**, *85*, 273-278.

[10] a) D. Bose, F. Meric-Bernstam, W. Hofstetter, D. A. Reardon, K. T. Flaherty, L. M. Ellis, *Lancet Oncol* **2010**, *11*, 373-382; b) C. G. Willett, Y. Boucher, E. di Tomaso, D. G. Duda, L. L. Munn, R. T. Tong, D. C. Chung, D. V. Sahani, S. P. Kalva, S. V. Kozin, M. Mino, K. S. Cohen, D. T. Scadden, A. C. Hartford, A. J. Fischman, J. W. Clark, D. P. Ryan, A. X. Zhu, L. S. Blaszkowsky, H. X. Chen, P. C. Shellito, G. Y. Lauwers, R. K. Jain, *Nat Med* **2004**, *10*, 145-147; c) S. Wilhelm, C. Carter, M. Lynch, T. Lowinger, J. Dumas, R. A. Smith, B. Schwartz, R. Simantov, S. Kelley, *Nat Rev Drug Discov* **2006**, *5*, 835-844; d) S. Sleijfer, I. Ray-Coquard, Z. Papai, A. Le Cesne, M. Scurr, P. Schoffski, F. Collin, L. Pandite, S. Marreaud, A. De Brauwer, M. van Glabbeke, J. Verweij, J. Y. Blay, *J Clin Oncol* **2009**, *27*, 3126-3132; e) L. Q. Chow, S. G. Eckhardt, *J Clin Oncol* **2007**, *25*, 884-896.

[11] S. Kim, D. Kim, H. H. Jung, I. H. Lee, J. I. Kim, J. Y. Suh, S. Jon, *Angew Chem Int Ed Engl* **2012**, *51*, 1890-1894.

[12] W. J. Fairbrother, H. W. Christinger, A. G. Cochran, C. Fuh, C. J. Keenan, C. Quan, S. K. Shriver, J. Y. K. Tom, J. A. Wells, B. C. Cunningham, *Biochemistry* **1998**, *37*, 17754-17764.

[13] H. W. C. W.J Fairbrother, A.G Cochran, G Fuh, C.J Keenan, C Quan, S.K Shriver, J.Y Tom, J.A Wells, B.C Cunningham, *Biochemistry* **1998**, *37*, 17754-17764.

[14] H. P. Gerber, X. Wu, L. Yu, C. Wiesmann, X. H. Liang, C. V. Lee, G. Fuh, C. Olsson, L. Damico, D. Xie, Y. G. Meng, J. Gutierrez, R. Corpuz, B. Li, L. Hall, L. Rangell, R. Ferrando, H. Lowman, F. Peale, N. Ferrara, *Proc Natl Acad Sci U S A* **2007**, *104*, 3478-3483.

[15] L. von Baumgarten, D. Brucker, A. Tirniceru, Y. Kienast, S. Grau, S. Burgold, J. Herms, F. Winkler, *Clin Cancer Res* **2011**, *17*, 6192-6205.

10.1002/anie.201811509

WILEY-VCH



**Entry for the Table of Contents**

## COMMUNICATION

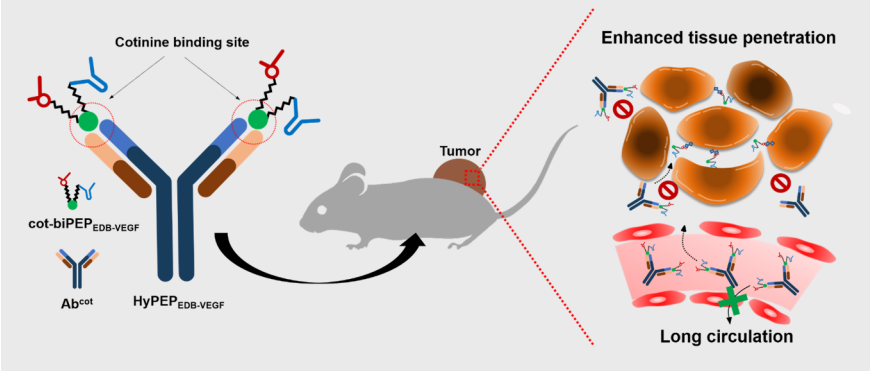


*B. Yu, D. Hwang, H. Jeon, H. Kim, Y. Lee, H. Keum, J. Kim, D.Y. Lee, Y. Kim, J. Chung, S. Jon**

***Page 1. – Page 5.***

**A Hybrid Platform Based on a Bispecific Peptide-antibody Complex for Targeted Cancer Therapy**

**Synergy in hybrid**-A new hybrid platform is developed based on a hapten-labeled bispecific peptide and an anti-hapten antibody to overcome the short plasma half-life of most peptide therapeutics.